Monitoring the Location, Amount, and Nature of Carbonaceous Deposits on Aged Zeolite Ferrierite Crystals by Using STEM-EELS

Sander van Donk,[a] Frank M. F. de Groot,[a] Odile Stéphan,[b] Johannes H. Bitter,[a] and Krijn P. de Jong*[a]

Abstract: By the use of electron energy-loss spectroscopy performed in a scanning transmission electron microscope (STEM-EELS), detailed spatial information is obtained concerning the amount and nature of carbonaceous deposits formed inside the crystals of the zeolite ferrierite (FER) during the reaction of *n*-butene to isobutene. In all cases, gradients in coke concentration over the crystal have been observed and quantified. An extensive accumulation of coke is observed at the entrance of the eight-membered-ring (MR) pores, while less coke is present at the entrances of the ten-MR channels. At a higher coke content, further filling up of the complete micropore system occurs and the eight-MR pores become fully blocked. The ten-MR channels remain partially accessible for *n*-butene, with alkyl-aromatic species deposited near the inlets of these channels. With regard to the selective transformation of *n*-butene into isobutene, this supports the view that the catalytic action takes place in the pore mouths of the ten-MR channels. Overall it is demonstrated that the major benefit of STEM-EELS is the possibility to simultaneously determine the position-resolved amount and nature of carbonaceous deposits on intact zeolite crystals.

Keywords: carbon · coke · ferrierite · STEM-EELS · zeolites

Introduction

Electron energy-loss spectroscopy (EELS) has proven to be a powerful technique in materials science and life sciences for detailed chemical characterization of nanosized structures.[1] Gallezot et al.[2] demonstrated the use of EELS for studying carbonaceous species deposited on the outer surface of various zeolite crystals by performing the measurements in a scanning transmission electron microscope (STEM-EELS). In this way it was demonstrated that the carbonaceous species blocked the entrance of the zeolite pores. Moreover, by interpretation of the carbon K-edge fine structure, the nature of the deposits was qualitatively resolved to be poly-aromatic.[2]

Carbonaceous deposits, often referred to as "coke", are generally known to provoke catalytic deactivation of zeolites.[3, 4] Besides deposition of coke at the outer surface, deactivation of zeolite catalysts may also be induced by carbonaceous species formed and deposited inside the zeolitic pore system. In that case the rate of deactivation and the location and nature of deposits inside the crystal is largely determined by the internal pore system of the zeolite.[5–7] Therefore, simultaneous determination of the location, amount, and nature of carbonaceous deposits may significantly contribute to the understanding of deactivation phenomena in zeolite catalysis induced by coking. As a result of recent technical developments STEM-EELS provides the possibility to obtain highly detailed spatial information, not only at the outer surface of a coked zeolite crystal as revealed by Gallezot et al.,[2] but also potentially inside the crystal. In this study it is demonstrated for the first time that by using STEM-EELS it is possible to unravel the influence of the pore structure on the coke deposition inside zeolite crystals. Additionally, by interpretation of the carbon K-edge fine structure an indication on the nature of the deposits is obtained.

The measurements are performed on crystals of the zeolite ferrierite (FER) that are aged during the catalytic conversion of *n*-butene into isobutene. FER consists of a two-dimensional pore network built up of ten-, eight-, six-, and five-membered rings (MR)[8] and is a highly suitable catalyst for the skeletal isomerization of *n*-butene into isobutene.[9] For this reaction the selective formation of isobutene coincides with the presence of carbonaceous deposits.[10–12] However, the exact

[a] Prof. K. P. de Jong, Dr. S. van Donk, Dr. F. M. F. de Groot, Dr. J. H. Bitter
Department of Inorganic Chemistry and Catalysis
Utrecht University, P.O. Box 80083
3508 TB Utrecht (The Netherlands)
Fax: +31 30-2511-027
E-mail: K.P.deJong@chem.uu.nl

[b] Dr. O. Stéphan
Laboratoire de Physique des Solides
Université Paris Sud
Bâtiment 510, 91405 Orsay (France)

DOI: 10.1002/chem.200204685

role of these deposits during the catalytic action is still under debate. Therefore, information about the location, amount, and nature of carbonaceous deposits in the zeolite crystals may contribute to a further understanding of the role of carbonaceous deposits in butene skeletal isomerization, and zeolite deactivation phenomena in general.

Results

Two FER samples with different amounts of carbonaceous deposits, exhibiting different catalytic properties, were prepared in a tapered element oscillating microbalance (TEOM). The first sample, obtained after 1 h on stream, contains 2.5 wt% coke (FER2.5C) and displays a high *n*-butene conversion, but a low selectivity to isobutene. The second sample, obtained after 300 h on stream, contains 6.8 wt% coke (FER6.8C) and is less active, but more selective towards isobutene. Their catalytic properties and micropore volumes as determined by nitrogen physisorption are summarized in Table 1.

By using STEM-EELS, the atomic carbon and oxygen signals were monitored for FER2.5C and FER6.8C, and the results as a function of the scanning distance in the directions parallel to the eight- (top) and ten-MR channels (bottom) are displayed in Figure 1. The first data points shown in the graphs are also the first points detected on the zeolite crystals. All performed line scans indicate that it takes about 50 Å before a stable oxygen signal is detected. The increasing oxygen signal suggests that the edges of the crystals are not entirely flat, but seem to be roughened in the direction perpendicular to the electron beam. Looking at the carbon signal, it becomes evident that a significant amount of carbonaceous species is deposited throughout the FER crystal. More carbonaceous deposits are present close to the pore mouths of the eight-MR rather than the ten-MR channels. This is evident from the fact that for both samples the carbon signal rises faster in the direction of the eight MR than the ten MR. The difference is particularly well illustrated in Figure 2, which shows line scans displaying the atomic carbon to zeolitic oxygen (C/O) ratios. These ratios are shown as a function of scanning distance parallel to the direction of the ten- and eight-MR channels for both FER2.5C (top) and FER6.8C (bottom). In the graphs, the origin represents the last data point detected just before the crystal, that is, in vacuum. The second data point in the graph is thus the first point detected on the zeolite crystal. Going from FER2.5C to FER6.8C, that is, with increasing coke content, the scans parallel to the eight-MR channels show a large increase in the C/O ratio at the crystal edge; this then declines going further into the crystal. In the direction of the ten-MR channels the C/O ratio also increases going from FER2.5C to FER6.8C, although more moderately.

Figure 3 zooms in on the C/O ratios detected further from the crystal edges, from 100 to 200 Å. For both FER2.5C (top)

Table 1. Catalytic properties and micropore volumes of the aged FER samples.

	FER2.5C	FER6.8C
time-on-stream [h]	1	300[a]
n-butene conversion [mol%]	81	24
isobutene selectivity [mol%]	20	87
isobutene yield [mol%]	16	22
micropore volume[b] [mL g^{-1}]	0.072	0.013

[a] After several hours on stream the maximum amount of deposits is reached. [b] Determined with N_2 physisorption, micropore volume for FER without deposits is 0.132 mL g^{-1}.

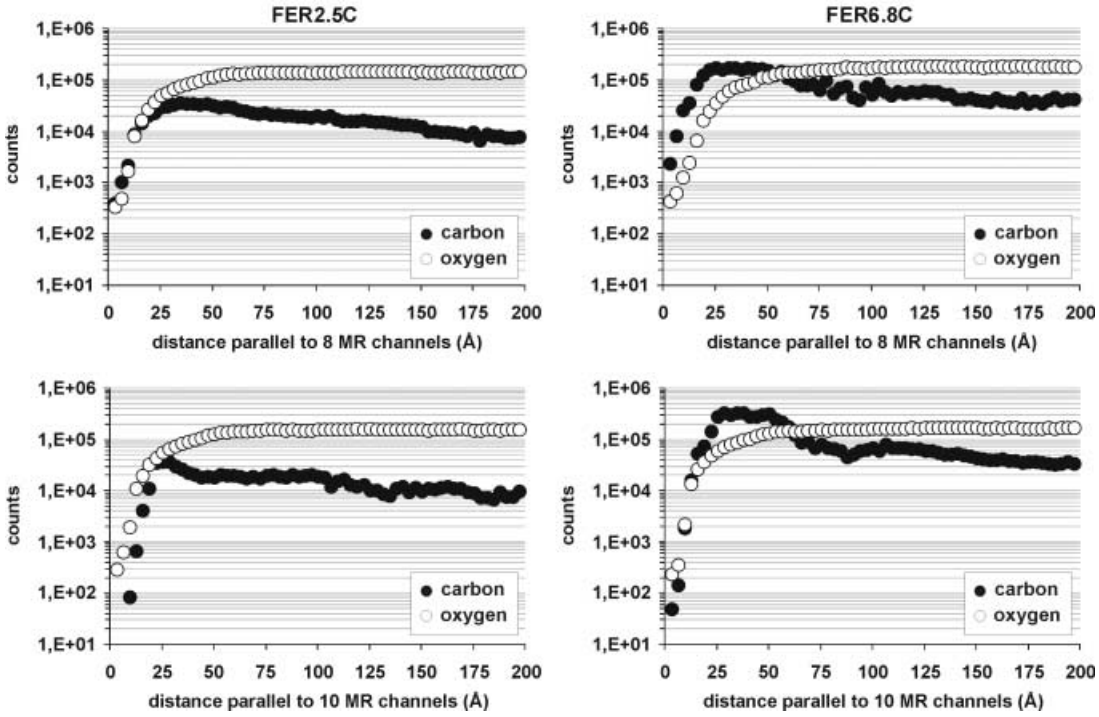

Figure 1. Carbon and oxygen signals for FER2.5C (left) and FER6.8C (right) as a function of scanning distance in the direction parallel to the eight- (top) and ten-MR channels (bottom). Note that the scale of the *y* axis is logarithmic.

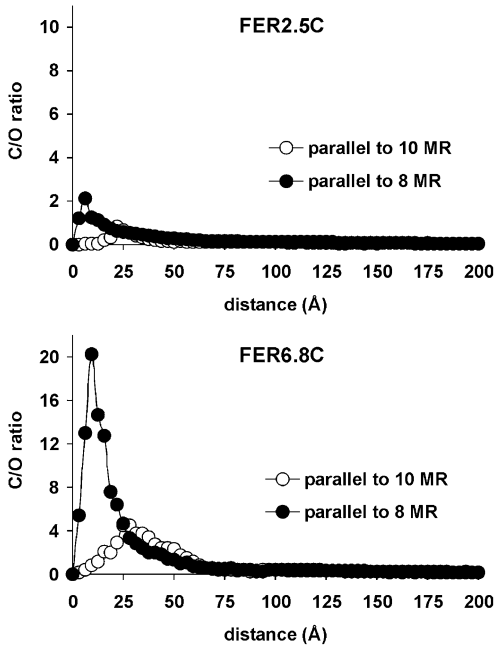

Figure 2. Atomic carbon to zeolitic oxygen ratios for FER2.5C (top) and FER6.8C (bottom) as a function of scanning distance. Line scans were taken parallel to the eight- and ten-MR channels, respectively. Note that there is a factor 2 difference in the *y* axis scale between the top and bottom graph.

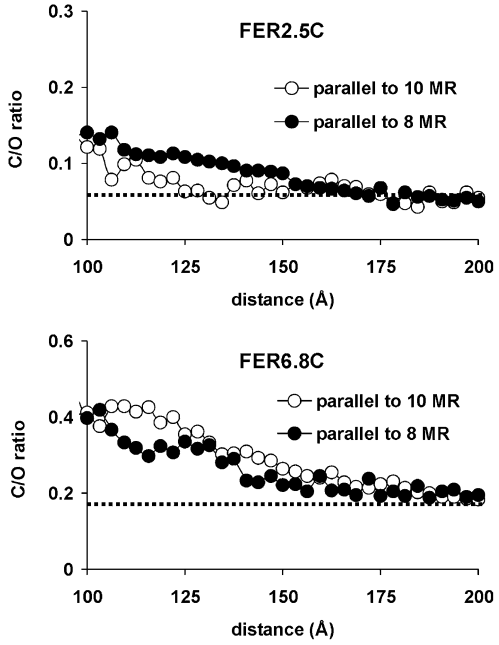

Figure 3. Atomic carbon to zeolitic oxygen ratios for FER2.5C (top) and FER6.8C (bottom) as a function of scanning distance from 100 to 200 Å. Line scans were taken parallel to the eight- and ten-MR channels, respectively. Dotted lines indicate the C/O ratio based on the overall coke content (see text). Note that there is a factor 2 difference in the *y* axis scale between the top and bottom graph.

and FER6.8C (bottom) a clear gradient in the C/O ratio is observed, which stabilizes at around 175 Å. The C/O ratio at this position coincides with the C/O ratio calculated from the bulk coke loading.

Figure 4 shows two-dimensional elemental maps for FER2.5C, which were obtained by combining a large number of parallel-recorded line scans. In this way Figure 4 provides a clear image of the carbon distribution over part of the mildly aged FER2.5C crystals. It is important to take into account that the results obtained for the first 50 Å are largely determined by the roughened planes of the FER crystal.

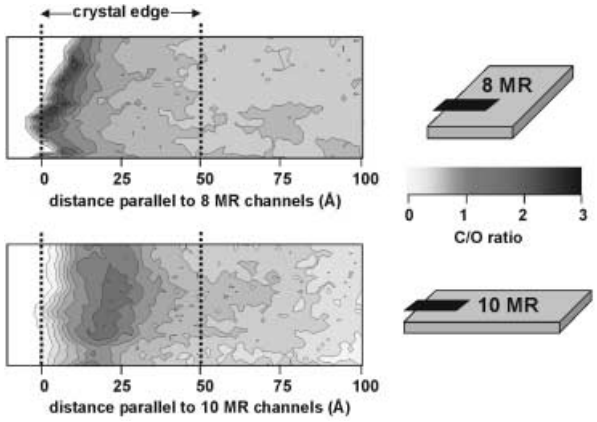

Figure 4. Two-dimensional elemental maps showing the atomic carbon to zeolitic oxygen (C/O) ratio over a representative crystal of FER2.5C, obtained by combining a large number of line scans parallel to the eight- (top) and ten-MR channels (bottom); the darker the area, the higher C/O ratio.

In Figure 5 the electron energy-loss spectra of the carbon K-edges detected at different locations in the FER6.8C crystals are displayed. The upper spectrum is obtained at ~20 Å from the edge of the crystal, that is, close to the pore

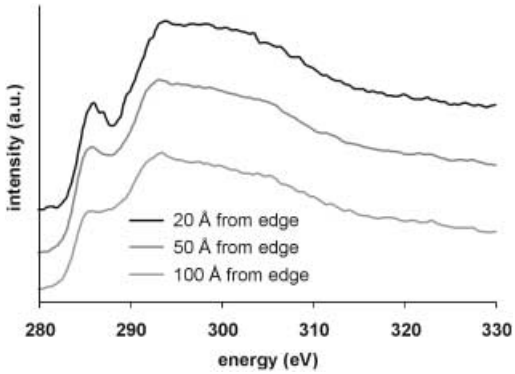

Figure 5. Carbon K-core edges for FER6.8C at various locations on the crystal, going from the edge at the ten-MR entrances (top spectrum) to the inside (bottom spectrum). For reasons of clarity we moved the baselines of the different spectra.

mouths of the ten-MR channels. The middle spectrum is obtained at ~50 Å and the bottom spectrum at ~100 Å from the crystal edge. To verify the nature of the carbonaceous species, the experimental spectra were evaluated using reference compounds.[13, 14] All carbon K-edges resemble the spectra of amorphous carbonaceous compounds, implying the presence of polyaromatic species. For all spectra obtained near the crystal edge, the leading peak is more distinct and an additional shoulder at 287 eV is visible, which is indicative for the presence aliphatic species and/or alkyl groups.

Discussion

The results displayed in Figure 1 show that for FER2.5C, that is, after 1 hour of *n*-butene reaction (see Table 1), there is carbon present at all distances scanned in both the eight- (top) and ten-MR (bottom) directions. This reveals that the reaction of *n*-butene results in an immediate deposition of carbonaceous species throughout the crystal. With regard to the oxygen signal, the line scans indicate that it takes about 50 Å before a stable oxygen signal is detected. This suggests that the edges of the crystals are not straight, but seem to be roughened in the direction perpendicular to the electron beam. At the same time, somewhat higher carbon signals are detected at the edges of the crystal in both the eight- and ten-MR directions, indicating that the pore mouths of both channels are sensitive to the deposition of carbonaceous deposits. Besides, by comparing the initial rise of the carbon signal with that of the oxygen signal, it becomes evident that the pore mouths of the eight-MR channels experience a more severe deposition of carbonaceous deposits than the inlets of the ten-MR channels. This is further illustrated in Figure 2 (top), which shows that for FER2.5C the maximum of the atomic C/O ratio is significantly higher at the entrance of the eight-MR channels than at the entrance of the ten-MR channels. Moreover, Figure 4 clearly visualizes that significant deposition of coke has occurred at the pore mouths of the eight-MR channels. Also at the entrances of the ten-MR channels some enrichment by coke species is observed; however, the location and amount indicate that the deposition has been less.

The higher sensitivity of the eight-MR channels towards the formation of coke may have two explanations. First, the diameter of an eight-MR channel is smaller than that of a ten-MR channel (see Figure 6). As a result the *n*-butene and/or

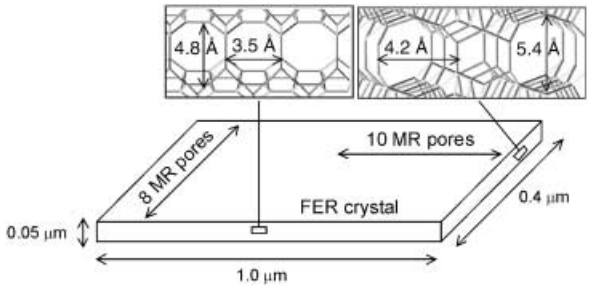

Figure 6. Schematic representation of a FER crystal, showing the average crystal-size and the directions and dimensions of the pores. Note: the kinetic diameter of *n*-butene is 3.0×4.7 Å.

the formed products will experience more steric hindrance in the eight-MR channels; this in turn causes accumulation of polymeric species that subsequently induce coke formation. Second, it has been demonstrated by infrared spectroscopy[12, 15] that the Brønsted acid sites in the eight-MR channels are located at slightly lower wavenumbers; this suggests that they might be more acidic and, therefore, more sensitive to irreversible deposition of carbonaceous species. Nevertheless, Figures 1, 2 (top), and 4 show that at the entrances of the ten-MR channels of FER2.5C some accumulation of carbonaceous species is also observed. Based on the nitrogen physisorption/t-plot analysis (Table 1), which reveals that there is still a significant amount of free micropore volume, it is suggested that the ten-MR channels of FER2.5C remain partially accessible.

For FER6.8C, obtained after 300 h *n*-butene reaction (see Table 1), Figures 1 and 2 (bottom) reveal a significant growth in the carbon signal throughout the crystal as compared to FER2.5C. Especially the considerable rise at the eight-MR pore inlets confirms the high sensitivity of these channels for the deposition of coke. The carbon signal at the edge of the ten-MR channels has also increased, but the slower growth indicates that the thickness and severity of the deposited coke layer is significantly less. Nitrogen physisorption/t-plot analysis for FER6.8C (Table 1) reveals that the micropore volume has decreased by a factor 10. Based on Figures 1 and 2 (bottom) it is suggested that this volume will be primarily located in the ten-MR pore entrances and that the eight-MR channels will be completely blocked. Overall, this implies that the ten-MR channels remain to some extent accessible for *n*-butene, even with a high coke content. With regard to the selective transformation of *n*-butene into isobutene over aged and selective FER, this suggests that the catalytic action will primarily occur in the initial part of the ten-MR channels.

Essential information concerning the filling of the FER micropore volume is provided by Figure 3, which zooms in on the C/O ratios detected further from the crystal edge. This demonstrates that inside the FER crystal a smooth carbon gradient is present that levels off around 175 Å. At a distance of 100 Å the C/O atomic ratio for FER2.5C is $\sim$0.14, which increases to $\sim$0.40 for FER6.8C. Going even further towards the center of the crystal at 200 Å from the crystal edge, the C/O atomic ratio for FER2.5C is $\sim$0.05 and for FER6.8C $\sim$0.18. The validity of these numbers can be verified by calculating the expected C/O ratios on the basis of elemental analysis. For this calculation, the chemical composition of FER2.5C can be represented as 2.5 wt% coke ("CH") and 97.5 wt% FER ("SiO_2"); this then leaves a C/O atomic ratio of $\sim$0.06. In a similar way FER6.8C can be represented as 6.8 wt% coke ("CH") and 93.2 wt% FER ("SiO_2"); this results in a C/O atomic ratio of $\sim$0.17. The theoretically obtained numbers agree very well with the experimentally observed ones obtained at 200 Å from the crystal edge. Regarding the fact that the size of the FER crystals under study is $\sim$10 000 Å (parallel to the ten MR) by $\sim$4000 Å (parallel to the eight MR), it is evident that the number for the bulk C/O ratio will be predominantly determined by the numbers detected at 200 Å from the crystal edge. For this reason, the higher C/O ratios detected at the crystal edges are of minor influence on the bulk C/O ratio of the crystal. The good agreement between theory and experiment indicates the sensitivity and validity of the STEM-EELS technique for establishing C/O ratios as a function of their location on aged zeolite crystals.

Having established the quantitative nature of the STEM-EELS C/O ratio, the coke enrichment close to the external surface of the FER crystals is considered. In view of the pore volume of FER ($0.13\,mL\,g^{-1}$) and a maximum density of polyaromatics in the pores of $\sim 1\,g\,mL^{-1}$, the intracrystalline coke loading cannot exceed $\sim$12 wt% corresponding to C/O

atomic ratio of ~0.3. This proves that the coke accumulation apparent in Figure 2 for both eight- and ten-MR-related crystal faces resides largely at the external surface of the crystal, in line with previous TEM results on aged FER.[11]

From the above discussion some indication is obtained on the growth of the coke going from FER2.5C to FER6.8C. The addition of reactants and/or products to the carbonaceous species already present will mainly occur through acid-catalyzed alkylation of butenes to aromatic coke in the initial part of the micropores, as is confirmed by the layer present at the crystal edges. In line with IR results[12] the eight-MR pores are coked up much more rapidly than the ten-MR pores. According to the STEM-EELS results, the intracrystalline coking reactions give rise to more extensive extracrystalline coke deposition. Next to the formation of an external coke layer, an intracrystalline coke gradient has been found (Figure 3). It is speculated that part of the butenes migrates further down into the zeolite channels, slowly increasing the overall C/O ratio inside the crystal. The above coke-deposition process is elaborated by Figure 5, which demonstrates that the carbonaceous species located around the C/O maximum in the ten-MR channels are both aromatic and aliphatic in nature, while the coke located further inside the crystal have been transformed into polyaromatic species. The nature of the coke on FER6.8C as detected by STEM-EELS is in good agreement with results obtained by infrared spectroscopy, revealing the presence of alkyl – aromatic species.[12, 16, 17] However, infrared spectroscopy is a bulk technique, while it is now demonstrated by STEM-EELS that the aromatic species with aliphatic groups present are predominantly located at the initial part of the ten-MR channels.

Conclusion

STEM-EELS measurements were performed on FER crystals aged during the skeletal isomerization of *n*-butene into isobutene. From this it is evident that carbonaceous species are deposited throughout the zeolite crystals. However, the carbon concentration is not uniform, since at the entrances of the eight-MR pores a large accumulation of coke is observed. For the ten-MR channels some enrichment by coke is also detected at the pore entrances. At a higher coke content, the micropores are further filled by carbonaceous species and the eight-MR pores become fully blocked. The ten-MR channels on the other hand remain partially accessible for *n*-butene, with alkyl – aromatic species deposited near the inlets of these channels. For this reason it is concluded that the selective transformation of *n*-butene into isobutene will take place in the primary part of the ten-MR channels. Overall, it is demonstrated that STEM-EELS is a powerful characterization technique for studying the location, amount, and nature of carbonaceous deposits in zeolite crystals.

Experimental Section

Sample preparation: Commercially available high silicon – NH_4^+ ferrierite (Zeolyst Int. Si/Al 30) with a crystal-size in the order of $1.0 \times 0.4 \times 0.05$ μm, as depicted in Figure 6, was activated in a dry nitrogen flow at 823 K for 12 h in order to obtain the H^+ ferrierite (H-FER). Nitrogen physisorption and t-plot analysis for H-FER showed an external surface area of 42 $m^2 g^{-1}$ and a micropore volume of 0.132 $mL g^{-1}$. Around 50 mg of FER (particle size: 90 – 150 μm) were aged during the *n*-butene (Hoek Loos, 1-butene, ≥ 99.5 %) reaction in a tapered element oscillating microbalance (TEOM, Rupprecht & Pataschnick 1500 PMA); reaction products were analyzed on-line using a gas chromatograph (Shimadzu 17A with a Chrompack PLOT capillary column of fused silica-Al_2O_3/KCL, 50 m × 0.32 mm). The TEOM reactor provided the possibility to study real-time catalyst deactivation induced by the deposition of carbonaceous deposits, while monitoring the catalytic reaction. For a detailed description of the TEOM we refer to work by Hershkowitz and Madiara,[18] and Chen et al.[19]

Two FER-samples with different amounts of carbonaceous deposits were prepared in the TEOM at 623 K, 1.3 bar using a weight hourly space velocity of 4 $g_{butene}\, g_{ferrierite}^{-1}\, h^{-1}$. The first sample, obtained after 1 h on stream, contained 2.5 wt % coke (FER2.5C). The second sample, obtained after 300 h on stream, contained 6.8 wt % coke (FER6.8C). Following the reactive adsorption of butenes, the samples were flushed at 623 K with nitrogen for 10 minutes followed by cooling down to ambient temperature.

STEM-EELS measurements: To investigate the carbon distribution on the aged H-FER crystals of FER2.5C and FER6.8C, carbon and oxygen K edges were monitored by use of a 100 keV STEM instrument (VG HB 501) equipped with a field emission source and a parallel Gatan 666 EELS spectrometer. The instrument was in operation in Orsay and produced EELS-spectra with 0.5 eV energy resolution and subnanometer spatial resolution within a typical acquisition time of a few hundreds of milliseconds per pixel. More specifically the subnanometer probe (typically 5 Å in diameter) could be positioned with an accuracy higher than 2 Å on the sample, and it could scan the sample digitally with spatial increments as small as 3 Å. For further details concerning the experimental set-up we refer to a report by Stéphan et al.[20] The aged H-FER crystals were first sonicated in ethanol and then dropped on a holey amorphous carbon film supported on a copper grid. Parts of the crystals protruding out into vacuum were selected for EELS investigation. The FER crystals used in this study were very appropriate for STEM-EELS measurements, since they were thin and platelike, as depicted in Figure 6. The two-dimensional pore network consisted of ten-MR channels with a size of 5.4×4.2 Å and eight-MR channels of 4.8×3.5 Å.[21] For both FER2.5C and FER6.8C one-dimensional line scans with a 5 Å probe size, 3.125 Å spatial increment, and 400 ms of exposure time were recorded by taking spectra while ramping the electron probe parallel to the eight- and ten-MR channels of the crystals. For FER2.5C a large number of parallel-recorded line scans were combined providing two-dimensional elemental maps. This was not possible for FER6.8C, since this sample was less stable in the electron beam. C/O atomic ratios were calculated after correction for the element sensitivities.[20]

Acknowledgement

This work was financially supported by the Netherlands Organization for Scientific Research (NWO/CW 700 – 97 – 019).

[1] C. Colliex, M. Tencé, E. Lefèvre, C. Mory, H. Gu, D. Bouchet, C. Jeanguillaume, *Mikrochim. Acta* **1994**, *114/115*, 71.
[2] P. Gallezot, C. Leclercq, M. Guisnet, P. Magnoux, *J. Catal.* **1988**, *114*, 100.
[3] P. Magnoux, P. Cartraud, S. Mignard, M. Guisnet, *J. Catal.* **1987**, *106*, 242.
[4] H. G. Karge, E. Boldingh, *Catal. Today* **1988**, *3*, 379.
[5] A. de Lucas, P. Canizares, A. Duran, A. Carrero, *Appl. Catal. A* **1997**, *156*, 299.
[6] A. R. Pradhan, J. F. Wu, S. J. Jong, W. H. Chen, T. C. Tsai, S. B. Liu, *Appl. Catal. A* **1997**, *159*, 187.
[7] H. S. Cerqueira, P. Magnoux, D. Martin, M. Guisnet, *Stud. Surf. Sci. Catal.* **1999**, *126*, 105.
[8] R. E. Morris, S. J. Weigel, N. J. Henson, L. M. Bull, M. T. Janicke, B. F. Chmelka, A. K. Cheetham, *J. Am. Chem. Soc.* **1994**, *116*, 11894.

[9] P. Grandvallet, K. P. de Jong, H. H. Mooiweer, A. G. T. G. Kortbeek, B. Kraushaar-Czarnetzki, European Patent no. 501577, **1992**, to Shell.
[10] W-Q. Xu, Y-G. Yin, S. L. Suib, C-L. O'Young, *J. Phys. Chem.* **1995**, *99*, 758.
[11] K. P. de Jong, H. H. Mooiweer, J. G. Buglass, P. K. Maarssen, *Stud. Surf. Sci. Catal.* **1997**, *111*, 127.
[12] S. van Donk, E. Bus, A. Broersma, J. H. Bitter, K. P. de Jong, *Appl. Catal. A* **2002**, *237*, 149.
[13] A. P. Hitchcock, D. C. Mancini, *J. Electron Spectrosc.* **1994**, *67*, 1.
[14] W. Teunissen, Ph. D. thesis, Utrecht University (NL), **2000**.
[15] L. Domokos, L. Lefferts, K. Seshan, J. A. Lercher, *J. Mol. Catal. A* **2000**, *162*, 147.
[16] P. Andy, N. S. Gnep, M. Guisnet, E. Benazzi, C. Travers, *J. Catal.* **1998**, *173*, 322.
[17] C. Pazè, B. Sazak, A. Zecchina, J. Dwyer, *J. Phys. Chem. B* **1999**, *103*, 9978.
[18] F. Hershkowitz, P. D. Madiara, *Ind. Eng. Chem. Res.* **1993**, *32*, 2969.
[19] D. Chen, A. Gronvold, H. P. Rebo, K. Moljord, A. Holmen, *Appl. Catal. A* **1996**, *137*, L1.
[20] O. Stéphan, A. Gloter, D. Imhoff, M. Kociak, K. Suenaga, M. Tencé, C. Colliex, *Surf. Rev. Lett.* **2000**, *7*, 475.
[21] *Atlas of Zeolite Framework Types*, 5th ed. (Eds.: Ch. Baerlocher, W. M. Meier, D. H. Olson), **2001**, Elsevier, Amsterdam.

Received: December 18, 2002 [F4685]

